# Astro2020 Science White Paper

## Spatially-resolved studies of star-forming galaxies in the reionization epoch

**Thematic Areas:** ☐ Planetary Systems ☐ Star and Planet Formation
☐ Formation and Evolution of Compact Objects ☑ Cosmology and Fundamental Physics
☐ Stars and Stellar Evolution ☑ Resolved Stellar Populations and their Environments
☑ Galaxy Evolution ☐ Multi-Messenger Astronomy and Astrophysics

**Principal Author:**
Name: Swara Ravindranath
Institution: Space Telescope Science Institute
Email: swara@stsci.edu
Phone: 410-338-2427

**Co-authors:**
Casey Papovich (Texas A&M University), Bethan James (STScI), Gregory Snyder (STScI), Anne Jaskot (UMass, Amherst), Henry Ferguson (STScI), Steve Finkelstein (UT Austin), Danielle Berg (Ohio State University), Mark Dickinson (NOAO), Jason Tumlinson (STScI), Taylor Hutchison (Texas A&M University), Marusa Bradac (UC Davis), Jeyhan Kartaltepe (Rochester Institute of Technology), Nimish Hathi (STScI), Dan Coe (STScI), Brett Salmon (STScI), Alaina Henry (STScI), Intae Jung (UT Austin)

**Abstract (optional):** Star-forming galaxies in the reionization epoch ($6 < z < 10$) harbor the signatures of early phases of galaxy assembly, involving gas accretion, star formation, chemical enrichment, growth of seed black holes, and the formation of the most massive, densest star clusters. The last decade witnessed unprecedented success in identifying large numbers of high redshift galaxies at z>6, and obtaining integrated spectra of some of the brightest, strongly-lensed galaxies. At $z > 6$, the rest-UV spectral features are redshifted to the near-infrared wavelengths, and serve as the main diagnostics to understand the ionizing spectrum, interstellar medium properties (such as, temperatures, densities, metal abundances), gas kinematics, and feedback processes. While integrated spectra can shed light on the global properties, spatially-resolved information is important to disentangle the interplay between star formation and black hole accretion, signatures of coherent gas motions, formation sites of compact stellar clusters, and evidence for outflows. Integral Field Spectrographs (IFS) that take advantage of the light-gathering power, and diffraction-limited performance of >20-meter class ground-based telescopes aided by adaptive optics (eg; GMT/TMT/E-ELT), or space-based missions (eg; LUVOIR) and can offer spatial resolutions $\leq$ 100 milli-arcseconds with spectral resolutions $R > 4000$ that will allow to unveil these important physical processes. **It is imperative that we harness these ground-breaking opportunities of the 2020s and provide the high spatial-resolution observations that are required to understand the true nature of galaxies in the era of reionizatio**n.

Over the last decade, deep imaging surveys have made an unprecedented impact to studies of star-forming galaxies in the reionization era by identifying large numbers of high redshift galaxies at z>6, with spectroscopic confirmation of redshifts available for a significant number of them (Finkelstein 2016; review). Taking advantage of the magnification offered by massive galaxy clusters that act as "cosmic lenses", has enabled the discovery of reionization sources at a time when the Universe was less than 500 Myrs old (Coe et al. 2013; Salmon et al. 2018). The next decade is poised to see another stage of dramatic progress through spatially-resolved spectroscopic studies of galaxies in the reionization epoch to understand the physical properties of their interstellar medium, metal abundances, kinematics, and outflows. At z>6, the rest-frame ultraviolet (UV) wavelengths are redshifted to the accessible near-IR wavelengths (0.9-2.5 micron), and the UV emission and absorption features serve as key diagnostics to study these properties. New spectral diagnostics based on UV nebular emission lines are being developed using photoionization models (Jaskot & Ravindranath 2016; Feltre et al. 2016, Byler et al. 2018). These diagnostics are being tested and calibrated against optical line diagnostics using samples of low-metallicity, dwarf galaxies at lower redshifts (Berg et al. 2016; Senchyna et al. 2017), so they can be applied to infer the properties of star-forming galaxies at z>6. In this white paper, we emphasize the science that is enabled by spatially-resolved rest-UV spectroscopy of galaxies in the reionization era, on physical scales of few 10-100 parsecs, to infer the nature of the ionizing sources, and the mechanisms that facilitate the escape of ionizing radiation. Such studies can be made possible with Integral Field Spectrographs (IFS) that take advantage of the light-gathering power and diffraction-limited performance of Extremely Large Telescopes ("ELTs"), such as the >20-meter class ground-based telescopes aided by adaptive optics (eg; GMT/TMT/E-ELT), or space-based missions (eg; LUVOIR).

# 1 Rest-UV nebular lines from reionization sources

Reionization ($6 \leq z \leq 10$) marks an important epoch of transition from a largely neutral to fully-ionized Universe. Star-forming galaxies (SFGs) are believed to be the primary sources of the ionizing radiation, but the production rate and the escape fraction of ionizing photons remains unclear (Finkelstein et al. 2019). The rest-UV spectra of SFGs provides a wealth of information about the shape of the ionizing spectrum, and physical properties of the surrounding ionized medium (such as, temperature, electron density, metal abundance, and kinematics) via the nebular emission lines arising from various ionized metal species. Among the most commonly observed UV emission lines in the high redshift SFGs, are Ly$\alpha\lambda$1216Å , CIV$\lambda\lambda$1548,1550Å , HeII $\lambda$1640Å , OIII]$\lambda\lambda$1661,1666Å , Si III]$\lambda\lambda$1883,1892Å, and CIII]$\lambda\lambda$1907,1909Å (Shapley et al. 2003; Steidel et al. 2016; Erb et al. 2010; Berg et al. 2018). Although, Ly$\alpha$ is the strongest emission line, it suffers progressively higher attenuation from the neutral intergalactic medium in the reionization epoch. The low-metallicity SFGs at $z \geq 6$ often exhibit strong CIII] emission with high equivalent widths (EWs), reaching $>$ 20Å in some cases (Stark et al. 2017; Hutchison et al. 2019). The higher ionization CIV emission has also been observed in SFGs at $z > 6$ (Stark et al. 2015; Mainali et al. 2017). The emergence of strong, high-ionization lines implies a transition to a harder ionizing spectrum at low-metallicities, and high ionization parameters (log $U \geq$ -2), which can only be successfully explained by incorporating new ingredients into the photoionization models, such as, the effects of binary star evolution (Jaskot & Ravindranath 2016, Steidel et al. 2016). The high ionization parameters also result in extreme emission lines in the

optical, such as [OIII]$\lambda\lambda$4959,5007Å with high EWs ($>$ 700Å) (Figure 1). In fact, the contribution of strong nebular [OIII]$\lambda$5007 to the Spitzer/IRAC mid-IR colors, is being increasingly used as a strategy to search for $z \sim 6.6 - 9.0$ galaxies with great success (Smit et al. 2015; Roberts-Borsani et al. 2016). The recent detections of the high ionization NV$\lambda$1243 emission in a $z > 7$ galaxies poses new challenges regarding the nebular emission, requiring AGNs or fast radiative shocks (Tilvi et al. 2016, Laporte et al. 2017; Mainali et al. 2018) to provide the necessary high energy photons.

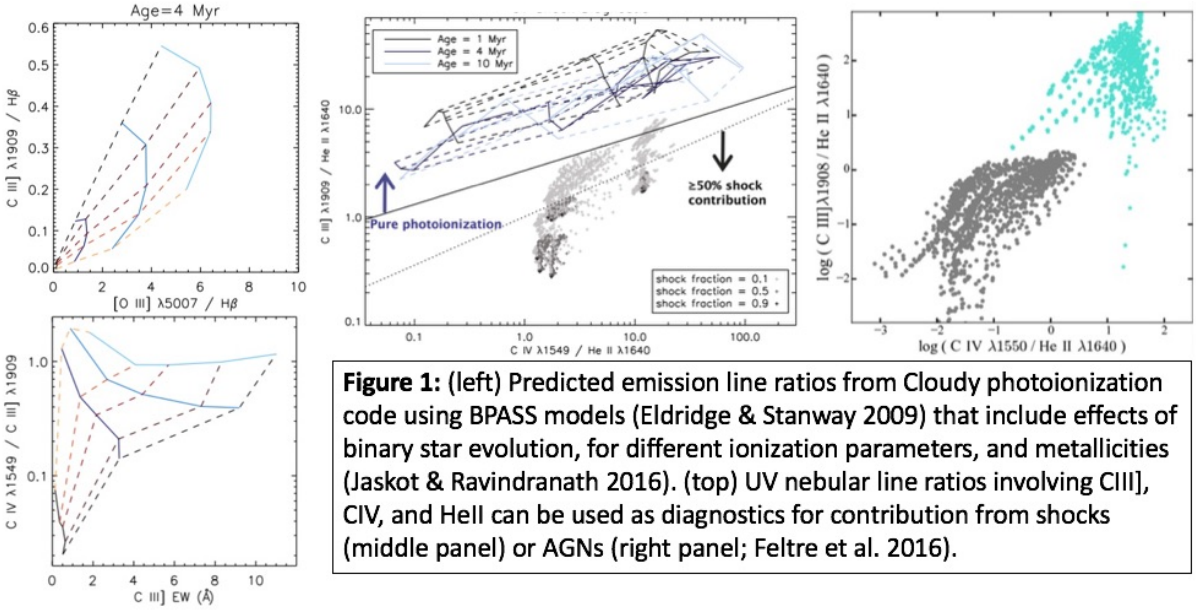


**Figure 1:** (left) Predicted emission line ratios from Cloudy photoionization code using BPASS models (Eldridge & Stanway 2009) that include effects of binary star evolution, for different ionization parameters, and metallicities (Jaskot & Ravindranath 2016). (top) UV nebular line ratios involving CIII], CIV, and HeII can be used as diagnostics for contribution from shocks (middle panel) or AGNs (right panel; Feltre et al. 2016).

# 2 UV spectral diagnostics to probe the nature of ionizers, gas kinematics, and outflows

The "BPT"-diagram (Baldwin et al. 1981) serves as an excellent diagnostic tool using rest-optical emission lines to understand the nature of ionizing sources in galaxies, the role of Active Galactic Nuclei (AGNs), and shocks. However, optical emission-lines redshift out of the near-IR wavelengths for the reionization sources, and it has become important to construct similar diagnostics using the UV emission-lines. The predicted line ratios from photoionization models show that diagnostic line ratios that use the CIV, He II, and CIII lines (Figure 1) can distinguish star-forming galaxies from AGNs (Feltre et al. 2016), and the contribution of shocks (Jaskot & Ravindranath 2016). The ratio of the high ionization metal lines (eg; CIV/CIII]) inform about the ionization parameter, and He II can be enhanced by shocks. The Si III] and CIII] emission doublets serve as electron density indicators (James at el. 2018; Maseda et al. 2017). The OIII]$\lambda\lambda$1661,1666Å, and CIII]$\lambda\lambda$1907,1909Å lines can probe the metal abundance (C/O ratio) in the gas (Berg et al. 2016; 2018), providing clues about the evolution of CNO at the earliest phases of galaxy formation, and to understand the interplay between star formation, supernovae feedback, and gas accretion.

At optical wavelengths, the H$\alpha$ recombination line is one of the strongest emission line features in the spectrum of star-forming galaxies and is widely used to map the gas kinematics. In the UV, the strongest is Ly$\alpha$ emission which is often extended compared to the continuum-emitting

region, and other nebular line emissions (Figures 2 and 3). Ly$\alpha$ radiation undergoes multiple scatterings in the surrounding neutral gas, and hence the Ly$\alpha$ profiles are modified by the relative velocities in the scattering medium, which makes it non-ideal for gas kinematics. However, Ly$\alpha$ profiles offer extremely valuable information about the neutral medium surrounding the continuum source, whether it is a static medium or shows evidence for gas infall/outflows (Djikstra 2014; Verhamme et al. 2015). CIII] is the next strongest UV emission line, reaching EW(CIII]) $> 20$Å in $z > 6$ galaxies, and therefore shows great promise for measuring the gas kinematics in high redshift SFGs. CIII] emission maps the velocity of the nebular gas in the HII regions, and the velocity gradients seen in the CIII] do not necessarily match the Ly$\alpha$ velocity field (Figure 2). CIII] kinematics reflects similar velocity information as would be obtained from H$\alpha$ emission or from Ly$\alpha$ if it were not resonantly-scattered. For instance, in the case of the Cosmic Horseshoe galaxy at $z = 2.38$, the CIII] velocity map and the H$\alpha$ kinematical map show the same trends in velocity gradients (James et al. 2018).

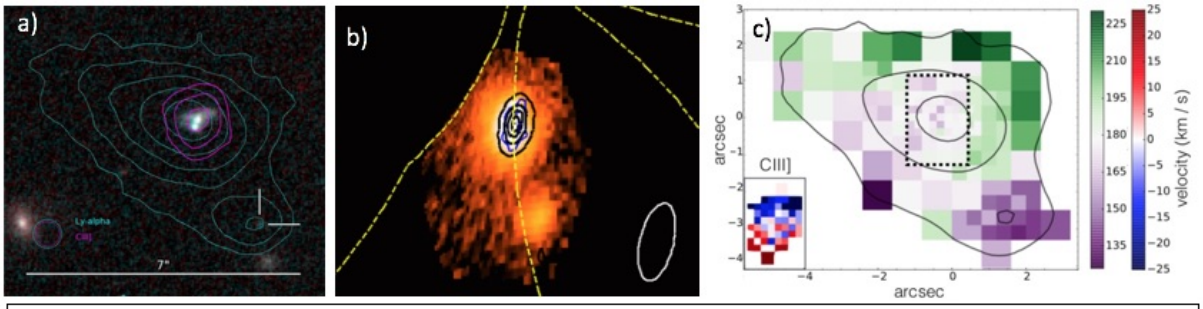


**Figure 2:** MUSE observations of one of the 5 multiple images of the strongly lensed young galaxy at z=3.5 the massive cluster SMACSJ2031.8-4036 (Patricio et al. 2016). (a) Ly$\alpha$ and CIII] contours overlaid on the HST continuum image, showing the extended nebular emission, and a Ly$\alpha$ emitting faint companion (white cross). (b) Source plane reconstruction of the Ly$\alpha$ emission, with CIII] emission shown as blue contours. Yellow dashed lines show the caustic lines and white ellipses show the source plane PSF. (c ) Ly$\alpha$ and CIII] velocity maps showing how CIII] maps gas kinematics while resonant scattering influences the frequency of Ly$\alpha$ photons.

Large-scale outflows at high-$z$ are universal, and identifiable via blue-shifted interstellar absorption by $\sim$100–300 km s$^{-1}$ in cool outflowing gas (e.g. Shapley et al. 2003; Steidel et al. 2010). Despite their ubiquity, there appears to be a wide range of properties in the absorption lines formed by outflowing gas. We are still essentially ignorant as to the underlying reasons for such diversity – differing covering fraction of the ISM, stellar age, or metallicity. Our knowledge is limited mostly by traditional methodology, where we integrate light over large spatial scales, making it extremely difficult to disentangle such properties. To date, only two studies have attempted to spatially resolve outflows beyond the local Universe, yielding contradictory results regarding the nature of outflowing gas (i.e. local vs. globally sourced, Bordoloi et al. 2016, James et al. 2018). In order to make progress, we need the ability to create deep, spatial maps of rest-UV outflowing signatures by harnessing the light of individual HII regions throughout SFGs.

# 3 Why is spatially-resolved spectra with IFS so crucial?

- IFS opens up the discovery space by enabling to see the "unexpected" – essentially going beyond sources selected for a specific program. For instance, VLT/MUSE observations

have revealed large numbers of pure-emission line sources, including Ly$\alpha$ emitters and CIII]-emitters through a blind search through the IFS datacube. (Smit et al. 2017)

- The nebular gas often shows extended emission, in particular, the Ly$\alpha$ emission can extend to significantly larger radii than the continuum emitting regions and the non-resonant nebular lines (Vanzella et al. 2017; Smit et al. 2017). This has implications for the energy source that powers the physical extent of the Ly$\alpha$ gas (Gronke & Bird 2017), and spatial variation of ISM properties within the SFGs. As such, it is imperative that we map and fully characterize this variation across the entire SFG.

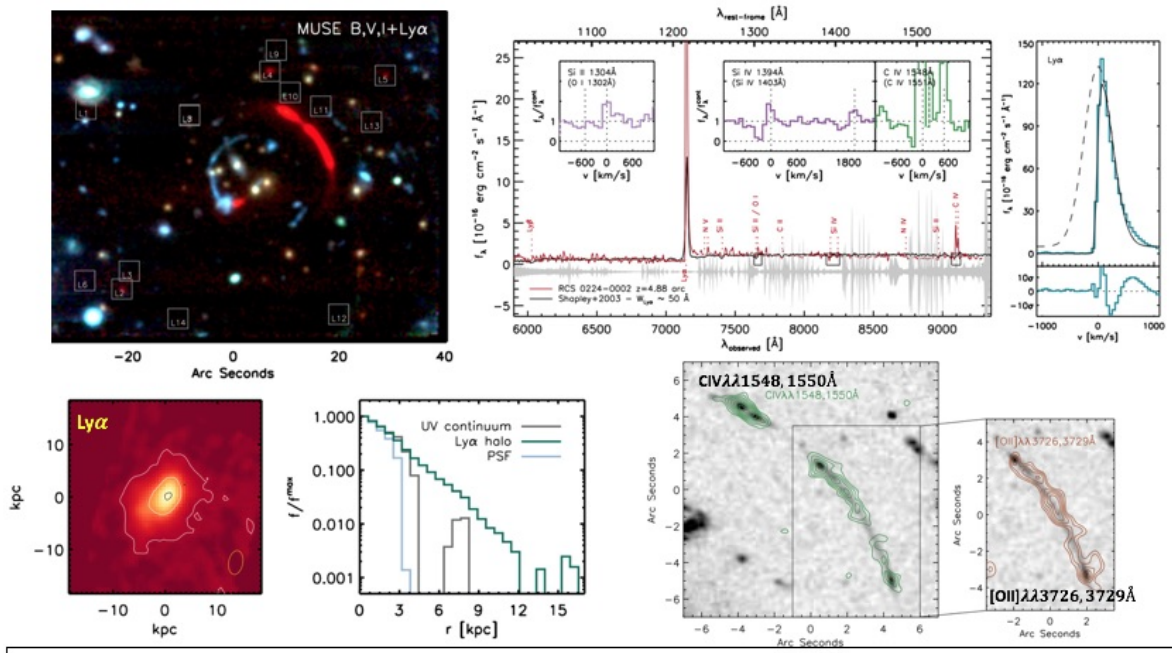


**Figure 3:** VLT-MUSE observations of the strongly-lensed z=4.88 emission-line galaxy behind the massive cluster RCS 0224 (Smit et al. 2017), along with the 1-D spectrum extracted over the region of the continuum, reveals the richness of IFS data to explore the UV emission and absorption features. The high spatial resolution offered by lensing offers emission-line maps of the extended Ly$\alpha$ emission, and the high-ionization metal emission lines of CIV and [OII].

- Obtaining the full kinematic information requires mapping the full extent of the gas emission. At $z > 6$, the earliest phases of galaxy assembly experiences strong outflows from the intense star formation activity within the SFGs, but there is also gas inflows through filamentary accretion, and mergers. Spatial velocity maps of the Ly$\alpha$ halo that extend beyond the continuum emission offer crucial insights into the interplay of gas infall (Vanzella et al. 2017) and star formation. Furthermore, spatially-resolved velocity information from CIII] is essential in exploring the gas dispersion and velocity gradients within the SFGs.

- The reionization epoch corresponds to a time of active star formation and black hole growth by gas accretion in young galaxies. Spatially resolved emission-line ratio maps offer the ability to disentangle the possible AGN signatures in the galaxy center from the global star formation through variation in the hardness of the radiation (via variation in the CIV/CIII] ratio, NV emission), and also to explore the first signs of metal abundance gradients (via the C/O ratios.)

- The ability to integrate light over individual star-forming regions enables robust determinations of the nature of the outflowing gas (i.e. velocity, covering fraction, metallicity) across SFGs at high-$z$. This can only be achieved by isolating single sightlines towards each region, and essentially uncontaminated interstellar absorption lines.

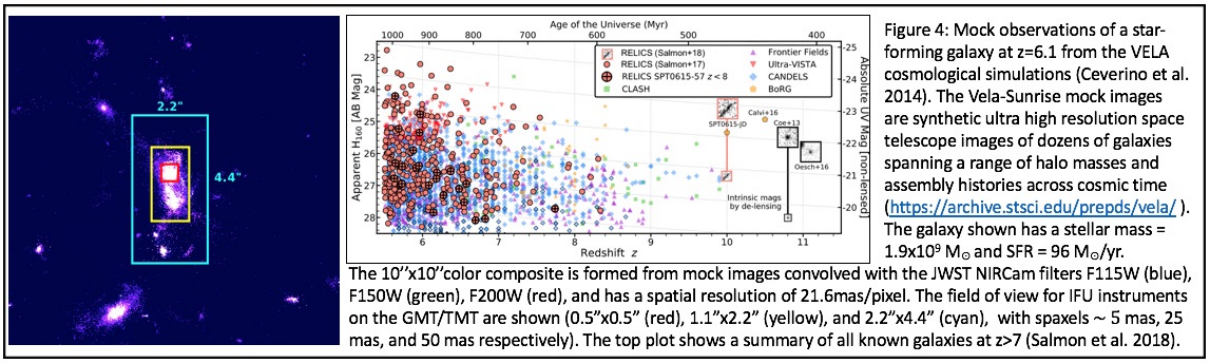


Figure 4: Mock observations of a star-forming galaxy at z=6.1 from the VELA cosmological simulations (Ceverino et al. 2014). The Vela-Sunrise mock images are synthetic ultra high resolution space telescope images of dozens of galaxies spanning a range of halo masses and assembly histories across cosmic time (https://archive.stsci.edu/prepds/vela/ ). The galaxy shown has a stellar mass = 1.9x10$^9$ M$_\odot$ and SFR = 96 M$_\odot$/yr. The 10''x10''color composite is formed from mock images convolved with the JWST NIRCam filters F115W (blue), F150W (green), F200W (red), and has a spatial resolution of 21.6mas/pixel. The field of view for IFU instruments on the GMT/TMT are shown (0.5"x0.5" (red), 1.1"x2.2" (yellow), and 2.2"x4.4" (cyan), with spaxels ~ 5 mas, 25 mas, and 50 mas respectively). The top plot shows a summary of all known galaxies at z>7 (Salmon et al. 2018).

# 4 Future of spatially-resolved studies of the reionization epoch

An IFS ($\lambda$ 0.9 - 2.5 $\mu$m) on large aperture (20-30 meter diameter) ground-based telescopes with adaptive optics (eg; GMT/TMT/E-ELT), and on space-based missions (eg; LUVOIR) will be essential to make dramatic progress in addressing the following questions regarding reionization: (1) AGNs and SFGs are both powered by gas accretion, and are likely to coexist at $z > 6$. Can we identify the AGN contribution by spatially-resolved mapping of the diagnostic line ratios?, (2) What is the dynamical state of gas around young galaxies as revealed by the Ly$\alpha$ velocity map? (3) Is there evidence for metal abundance (C/O) gradients in these early phases of galaxy assembly? (4) Is there evidence for coherent rotation in the gas kinematics from CIII] and other emission lines? (5) Using gravitationally-lensed arcs, can we identify super-star clusters and witness the formation of proto-globular clusters?. The sources to be targeted for spatially resolved studies at these redshifts ($6 \leq z \leq 10$) are very faint with observed magnitudes $>$ 28-31 AB magnitude in the NIR wavebands, and their effective radii are $<$ 100 mas (Holwerda et al. 2015; Kawamata et al. 2018). The IFU on JWST/NIRSPEC offers a spatial resolution $\sim$100 mas, and will not have the much needed resolution elements within the effective radius to distinguish central AGN signatures from global star formation, kinematics, or metal gradients in $z > 6$ galaxies. The emission-line fluxes (eg; CIII], CIV) are in the range $\sim 10^{-18} - 10^{-20}$ erg/s/cm$^2$ (Shimizu et al. 2016) requiring prohibitively long IFU exposures with JWST, unlike with the ELTs (Wright et al. 2010), and spectral resolution $R > 4000$ is required to measure the velocity dispersions ($\sigma \leq 60$ km/s). Most of the existing IFU observations at $z > 2$ have combined the power of the magnification offered by strong-gravitational lensing in massive galaxy clusters ("Cosmic Telescopes"), with the largest ground-based telescopes to study the resolved properties of lensed arcs of faint background galaxies. This strategy offers exquisite details in the few cases where such high magnification can be achieved. Future ELTs will enable IFS observations of well-defined galaxy samples reaching resolving physical scales of few 100 parsecs even in unlensed galaxies (Figure 4). In lensed systems, the IFS on ELTs will offer unprecedented opportunity to resolve scales of few tens of parsecs and explore the super-star clusters or proto-globular clusters (Vanzella et al. 2017).

**References**


Baldwin, J. A., Phillips, M. M., Terlevich, R. 1981, PASP, 93, 5
Berg, D. A., Skillman, E. D., Henry, R. B. C.; Erb, D. K., Carigi, L. 2016, ApJ, 827, 126
Berg, D.A., Erb, D. K., Auger, M. W., Pettini, M.,; Brammer, G. B. 2018, ApJ, 859, 164
Byler, N., Dalcanton, J. J., Conroy, C., Johnson, B. D. et al. 2018, ApJ, 863, 14
Ceverino, D., Klypin, A., Klimek, E. S. et al. 2014, MNRAS, 442, 1545
Coe, D., Zitrin, A., Carrasco, M., Shu, X., Zheng, W., Postman, M. 2013, ApJ, 762, 32
Dijkstra, M. 2014, PASA, 31, 40
Eldridge, J.J. & Stanway, E. 2009,MNRAS, 400, 1019
Erb, D. K., Pettini, M., Shapley, A. E., Steidel, C. C. et al. 2010, ApJ, 719, 1168
Feltre, A., Charlot, S., Gutkin, J. 2016, MNRAS, 456, 3354 Finkelstein, S. L. 2016, PASA, 33, 37
Finkelstein et al. 2019, arXiv:1902.02792
Gronke, M., & Bird, S. 2017, ApJ, 835, 207 Holwerda, B.W., Bouwens, R., Oesch, P.A., Smit, R. et al. 2015, ApJ, 808, 6
Hutchison, T. A., Papovich, C., Finkelstein, S., et al. 2019, ApJ (submitted)
Jaskot, A.-E. & Ravindranath, S. 2016, ApJ, 833, 136
James, B. L., Auger, M., Pettini, M., Stark, D. P., et al., S. 2018, MNRAS, 476, 1726
Kawamata, R., Ishigaki, M., Shimasaku, K., et al. 2018, ApJ, 855, 4
Laporte, N., Nakajima, K., Ellis, R. S., Zitrin, A., Stark, D. P. et al. 2017, ApJ, 851, 40
Maseda, M. V.,Brinchmann, J., Franx, M., Bacon, R., Bouwens, R.J. et al. 2017, A&A., 608, 4
Mainali, R. Kollmeier, J. A., Stark, D. P., Simcoe, R. A., Walth, G. et al. 2017, ApJ, 836,14
Mainali, R., Zitrin, A., Stark, D. P., Ellis, R. S., Richard, J. et al. 2018, MNRAS, 479, 1180
Patricio, V., Richard, J., Verhamme, A., Wisotzki, L., et al. 2016, MNRAS, 456, 4191
Roberts-Borsani, G. W., Bouwens, R. J., Oesch, P. A., et al. 2016, ApJ, 823, 143
Salmon, B., Coe, D., Bradley, L., Bradac, M., et al. 2018, ApJ, 864, 22
Shimizu, I., Inoue, A. K., Okamoto, T., Yoshida, N. 2016, MNRAS, 461, 3563
Senchyna, P., Stark, D. P., Vidal-Garcia, A., Chevallard, J., et al. 2017, MNRAS, 472, 2608
Smit, R., Swinbank, A. M., Massey, R., Richard, J., et al.. 2017, MNRAS, 467, 3306
Smit, R., Bouwens, R. J. Franx, M., Oesch, P. A. et al. 2015, ApJ, 801, 122
Shapley, A.E., Steidel, C.C., Pettini, M., Adelberger, K. L., 2003, ApJ, 588, 65
Steidel, C.C., Strom, A. L., Pettini, M., Rudie, G. C., Reddy, N. A., et al. 2016, ApJ, 826,159
Stark, D. P., Walth, G., Charlot, S., Cl'ement, B., Feltre, A., et al. 2015, MNRAS, 454, 1393
Stark, D. P., Ellis, R. S., Charlot, S., Chevallard, J., Tang, M. et al. 2017, MNRAS, 464, 469
Tilvi, V.; Pirzkal, N.; Malhotra, S.; Finkelstein, S. L.; Rhoads, J. E.; et al. 2016ApJ...827L..14T
Vanzella, E., Balestra, I., Gronke, M., Karman, W. et al. 2017, MNRAS, 465, 3803
Vanzella, E., Castellano, M., Meneghetti, M., Mercurio, A. et al. 2017, ApJ, 842, 47
Verhamme, A., Orlitova, I., Schaerer, D., Hayes, M. 2015, A&A, 578, A7
Wright, S. Barton, E.J., Larkin, J.E., Moore, A.M. et al. 2010, SPIE, 7735, 7